Measurement of nanometric displacements by correlating two speckle interferograms

ARTICLE *in* APPLIED OPTICS · APRIL 2011

Impact Factor: 1.78 · DOI: 10.1364/AO.50.001758 · Source: PubMed

4 AUTHORS, INCLUDING:

Lucas P. Tendela
National Scientific and Technical Research …
6 PUBLICATIONS **13** CITATIONS
SEE PROFILE

Gustavo Galizzi
Instituto de Física Rosario
41 PUBLICATIONS **448** CITATIONS
SEE PROFILE

Guillermo H Kaufmann
Instituto de Física Rosario
172 PUBLICATIONS **1,733** CITATIONS
SEE PROFILE

Measurement of nanometric displacements by correlating two speckle interferograms

Lucas P. Tendela,[1,*] Gustavo E. Galizzi,[1] Alejandro Federico,[2] and Guillermo H. Kaufmann[1,3]

[1]Instituto de Física Rosario, Blvd. 27 de Febrero 210 bis, S2000EZP Rosario, Argentina

[2]Electrónica e Informática, Instituto Nacional de Tecnología Industrial, P.O. Box B1650WAB, B1650KNA San Martín, Argentina

[3]Centro Internacional Franco Argentino de Ciencias de la Información y de Sistemas, Blvd. 27 de Febrero 210 bis, S2000EZP Rosario, Argentina

*Corresponding author: tendela@ifir-conicet.gov.ar

Received 14 December 2010; revised 15 February 2011; accepted 24 February 2011; posted 2 March 2011 (Doc. ID 139602); published 15 April 2011

This paper presents a method to measure nanometric displacement fields using digital speckle pattern interferometry, which can be applied when the generated correlation fringes show less than one complete fringe. The method is based on the evaluation of the correlation between the two speckle interferograms generated by both deformation states of the object. The performance of the proposed method is analyzed using computer-simulated speckle interferograms. A comparison with the performance given by a phase-shifting technique is also presented, and the advantages and limitations of the proposed method are discussed. Finally, the performance of the proposed method to process real data is illustrated.

OCIS codes: 120.6160, 120.2650, 120.4630, 120.5050.

1. Introduction

The rapid miniaturization of microelectromechanical systems (MEMS), microsensors, and micro-optical devices, such as mirror matrices, has raised new challenges in the development of nondestructive and noncontact testing methods. The reason for this demand is that properties determined on much larger specimens cannot be scaled down from bulk materials without any experimental verification. This affirmation is also based on the fact that the material behavior of most microsystems in combination with new structural designs cannot be easily predicted by numerical simulations. Therefore, there exists a considerable demand for measurement techniques to test these systems, not only in the development phase but also during the entire manufacture process, even at the wafer scale.

Whole-field optical techniques provide a promising alternative to conventional inspection methods, as they are fast, robust, noncontact, and nondestructive [1]. These methods also present high sensitivity and accuracy, high resolution of data points, and the possibility of automating data analysis. Among these inspection techniques, we can mention digital speckle pattern interferometry (DSPI), which is a well-known coherent optics technique that is widely used for whole-field measurement of displacement and strain fields, and contours in rough object surfaces [2]. DSPI is based on the determination of optical phase changes by the acquisition of speckle interferograms produced by different deformation states of a specimen, which are correlated to generate fringe patterns. The most common approach used in DSPI to produce the correlation fringes is to subtract two speckle interferograms, so that patterns with good

0003-6935/11/121758-07$15.00/0

visibility can be generated. A review of recent applications of DSPI to microsystem inspection can be found in Ref. [3].

To retrieve phase distributions in DSPI, the phase-shifting and the Fourier transform methods are the most commonly used approaches [4]. As it is well known, phase-shifting methods, which are based on the processing of two sets of three or more phase-shifted speckle interferograms, offer a number of advantages. Perhaps the most important ones are their high accuracy and that the sign ambiguity is resolved automatically due to the recording of multiple interferograms. However, the price that one has to pay for these advantages is the additional technical complexity that must be introduced in the optical setup. For example, these algorithms assume that phase shifts between successive frames are all equal, which can be difficult to obtain experimentally. Nonlinearities in the photodetector, phase-shifter miscalibrations, and vibrations during the acquisition of the multiple speckle interferograms also produce systematic errors that must be appropriately addressed [5,6].

On the other hand, the Fourier transform method has the advantage of requiring the acquisition of only two speckle interferograms. Nevertheless, when phase changes are nonmonotonic, this method needs the introduction of spatial carrier fringes to overcome the sign ambiguity [4]. Although there exist simple ways of introducing spatial carrier fringes in the optical setup, such as tilting the reference beam between the acquisition of both speckle interferograms to be correlated, this procedure also complicates the automation of the interferometer operation.

Since the invention of DSPI, various authors have reported on different methods based on the use of correlation coefficients to calculate speckle correlation fringe patterns [7,8]. An alternative method based on the Pearson's correlation coefficient was used in Ref. [9] to estimate the local correlation between two speckle patterns acquired before and after translation of an object. The main advantage of this approach is that the illumination over the surface of the object need not be perfectly uniform. Therefore, the correlation coefficient calculated is automatically normalized over the entire fringe pattern, allowing the method to be used under poor illumination conditions. However, this approach has the disadvantage that the calculations to carry out the correlation require more computational effort than is needed for the frame subtraction method.

In this paper, we propose a novel phase evaluation method to be used in DSPI, when this technique is applied for the measurement of nanometric displacements in cases where the correlation fringes show less than one complete fringe. To our knowledge, in none of the previously published works has a correlation coefficient been used to evaluate phase distributions, as is done here. The case of a correlation fringe pattern presenting less than one complete fringe can appear quite frequently when microsystems are inspected. In this case, the phase change generated by the deformation is less than π, so that the wrapped phase map does not present the usual 2π phase discontinuities and it is not necessary to apply a spatial phase unwrapping algorithm to obtain the continuous phase distribution.

The proposed phase evaluation method is based on the calculation of the correlation between the two speckle interferograms generated by both deformation states of the object. After describing the fundamentals of the proposed method, its performance is analyzed using computer-simulated speckle interferograms, an approach that allows us to know precisely the original phase distribution and also to evaluate the rms phase error. A comparison with the performance given by the Carré phase-shifting algorithm [4] is also presented, and the advantages and limitations of the proposed method are discussed. Finally, the performance of the proposed method to process real data is illustrated.

2. Theoretical Concepts

The resulting intensity I of the superposition of two coherent optical fields having intensities I_1 and I_2 in a given spatial coordinate is determined by the well-known relation

$$I = I_1 + I_2 + 2\sqrt{I_1 I_2}\cos(\phi_1 - \phi_2) = I_0 + I_M \cos\phi, \tag{1}$$

where $I_0 = I_1 + I_2$ is the intensity bias, $I_M = 2\sqrt{I_1 I_2}$ is the modulation intensity, and ϕ_1 and ϕ_2 are the phases of the complex optical fields associated with I_1 and I_2, respectively. $\phi = \phi_1 - \phi_2$ accounts for the optical path difference from the light source to the observation point considered [2].

In the case of the DSPI technique, at least one of the optical waves is a speckle field generated by the scattered light coming from an optically rough surface. As it is well known, the superposition of both optical waves produces another speckle field called an interferogram, in which I_0, I_M, and ϕ vary randomly and rapidly in space. If the scattering surface undergoes a deformation, the resulting intensity changes accordingly. In this case, the detected intensities I_a and I_b corresponding to the initial and deformed states, respectively, can be determined from Eq. (1) as

$$\begin{aligned} I_a &= I_{a0} + I_{aM}\cos\phi_a = I_{a0} + I_{aM}\cos\phi_s, \\ I_b &= I_{b0} + I_{bM}\cos\phi_b = I_{b0} + I_{bM}\cos(\phi_s + \Delta\phi), \end{aligned} \tag{2}$$

where $\phi_s = \phi_a$ accounts for the random change in the optical path due to the roughness of the scattering surface and $\Delta\phi = \phi_b - \phi_a$ corresponds to the deterministic change in the path introduced by the undergone deformation.

Below we present a relationship to characterize the deterministic phase change $\Delta\phi$ as a function of the Pearson's correlation coefficient between the

two interferograms described by Eq. (2), taking into account the general hypothesis about the speckle distribution generated by the rough object. The Pearson's correlation coefficient $C(p,q)$ between two random variables p and q is defined as the covariance of the two variables divided by the product of their standard deviations and can be estimated as [10]

$$C(p,q) = \frac{\langle (p - \langle p \rangle)(q - \langle q \rangle) \rangle}{[(\langle p^2 \rangle - \langle p \rangle^2)(\langle q^2 \rangle - \langle q \rangle^2)]^{1/2}}, \tag{3}$$

where $\langle\rangle$ stands for the mean value of the sampled random variable.

In the case of the two recorded interferograms I_a and I_b, the correlation coefficient $C(I_a - I_{a0}, I_b - I_{b0})$ is given by

$$\begin{aligned} C &= \frac{\langle (I_a - I_{a0} - \langle I_a - I_{a0} \rangle)(I_b - I_{b0} - \langle I_b - I_{b0} \rangle) \rangle}{[(\langle (I_a - I_{a0})^2 \rangle - \langle I_a - I_{a0} \rangle^2)(\langle (I_b - I_{b0})^2 \rangle - \langle I_b - I_{b0} \rangle^2)]^{1/2}} \\ &= \frac{\langle (I_{aM} \cos\phi_a - \langle I_{aM} \cos\phi_a \rangle)(I_{bM} \cos\phi_b - \langle I_{bM} \cos\phi_b \rangle) \rangle}{[(\langle I_{aM}^2 \cos^2\phi_a \rangle - \langle I_{aM} \cos\phi_a \rangle^2)(\langle I_{bM}^2 \cos^2\phi_b \rangle - \langle I_{bM} \cos\phi_b \rangle^2)]^{1/2}}, \end{aligned} \tag{4}$$

where Eq. (2) was used and the operator $\langle\rangle$ is evaluated by using a sliding window technique on each recorded image. The reader should note that the spatial coordinates of the pixel (m,n) at the CCD for $m,n = 1,\ldots,L$, where L is the number of pixels along the horizontal and vertical directions, were omitted intentionally.

Considering that $\Delta\phi$ is a deterministic magnitude, after some mathematical manipulations the numerator N_{ab} of Eq. (4) can be expressed as a function of $\cos\Delta\phi$ and $\sin\Delta\phi$:

$$\begin{aligned} N_{ab} &= \langle (I_{aM}\cos\phi_a - \langle I_{aM}\cos\phi_a \rangle) \\ &\quad \times (I_{bM}\cos\phi_b - \langle I_{bM}\cos\phi_b \rangle) \rangle \\ &= \langle (I_{aM}\cos\phi_s - \langle I_{aM}\cos\phi_s \rangle)(I_{bM}\cos\phi_s \\ &\quad - \langle I_{bM}\cos\phi_s \rangle)\cos\Delta\phi - (I_{aM}\cos\phi_s \\ &\quad - \langle I_{aM}\cos\phi_s \rangle)(I_{bM}\sin\phi_s \\ &\quad - \langle I_{bM}\sin\phi_s \rangle)\sin\Delta\phi \rangle. \end{aligned} \tag{5}$$

Assuming that the intensity and phase of the fully developed and polarized speckle fields are statistically independent, the following relationships are valid:

$$\begin{aligned} \langle I_M \cos\phi_s \rangle &= \langle I_M \rangle \langle \cos\phi_s \rangle, \\ \langle I_M \sin\phi_s \rangle &= \langle I_M \rangle \langle \sin\phi_s \rangle, \\ \langle I_M^2 \sin^2\phi_s \rangle &= \langle I_M^2 \cos^2\phi_s \rangle, \\ \langle \sin\phi_s \rangle &= \langle \cos\phi_s \rangle \approx 0, \\ \langle \sin\phi_s \cos\phi_s \rangle &\approx 0. \end{aligned} \tag{6}$$

By using the set of relations given by Eq. (6), the numerator N_{ab} can be approximated by

$$N_{ab} \approx \langle I_{aM} I_{bM} \cos^2\phi_s \rangle \cos\Delta\phi. \tag{7}$$

In a similar way, the denominator D_{ab} of Eq. (4) can be expressed as

$$\begin{aligned} D_{ab} &= [(\langle I_{aM}^2 \cos^2\phi_a \rangle - \langle I_{aM}\cos\phi_a \rangle^2)(\langle I_{bM}^2 \cos^2\phi_b \rangle \\ &\quad - \langle I_{bM}\cos\phi_b \rangle^2)]^{1/2} \\ &= \{(\langle I_{aM}^2 \cos^2\phi_s \rangle \\ &\quad - \langle I_{aM}\cos\phi_s \rangle^2)[\langle I_{bM}^2 (\cos\phi_s \cos\Delta\phi \\ &\quad - \sin\phi_s \sin\Delta\phi)^2 \rangle \\ &\quad - \langle I_{bM}(\cos\phi_s \cos\Delta\phi - \sin\phi_s \sin\Delta\phi) \rangle^2]\}^{1/2}. \end{aligned} \tag{8}$$

Considering the relationships expressed in Eqs. (6), the denominator D_{ab} can be approximated by

$$\begin{aligned} D_{ab} &\approx [\langle I_{aM}^2 \cos^2\phi_s \rangle (\langle I_{bM}^2 \cos^2\phi_s \rangle \cos^2\Delta\phi \\ &\quad + \langle I_{bM}^2 \sin^2\phi_s \rangle \sin^2\Delta\phi)]^{1/2} \\ &= [\langle I_{aM}^2 \cos^2\phi_s \rangle \langle I_{bM}^2 \cos^2\phi_s \rangle]^{1/2}. \end{aligned} \tag{9}$$

By replacing Eqs. (7) and (9) into Eq. (4), the correlation coefficient C can be estimated as

$$C(I_a - I_{a0}, I_b - I_{b0}) \approx \frac{\langle I_{aM} I_{bM} \cos^2\phi_s \rangle \cos\Delta\phi}{[\langle I_{aM}^2 \cos^2\phi_s \rangle \langle I_{bM}^2 \cos^2\phi_s \rangle]^{1/2}}. \tag{10}$$

Also, it should be noted that, due to the independence between the intensity and the phase, $\langle \cos^2\phi_s \rangle$ can be canceled out in Eq. (10), to obtain the following simple relationship between the correlation coefficient C and $\cos\Delta\phi$:

$$C(I_a - I_{a0}, I_b - I_{b0}) = \frac{\langle I_{aM} I_{bM} \rangle}{\sqrt{\langle I_{aM}^2 \rangle \langle I_{bM}^2 \rangle}} \cos\Delta\phi. \tag{11}$$

It is important to also note that $\langle \cos^2\phi_s \rangle$ is not a vanishing contribution and that Eq. (11) is valid independently of the statistical nature that follows the random phase, although the relationships in Eq. (6) should be satisfied. Finally, the phase change $\Delta\phi$ needed to determine the displacement components

can be evaluated by inverting Eq. (11) as follows:

$$\Delta\phi = \operatorname{acos}\left[C(I_a - I_{a0}, I_b - I_{b0})\frac{\sqrt{\langle I_{aM}^2\rangle\langle I_{bM}^2\rangle}}{\langle I_{aM} I_{bM}\rangle}\right], \quad (12)$$

where acos[] is the inverse of the cosine function.

As previously mentioned, this technique can be applied for the measurement of nanometric displacements in cases where the correlation fringes show less than one complete fringe. Therefore, as the wrapped phase distribution does not present the usual 2π phase discontinuities, it is not necessary to apply a spatial phase unwrapping algorithm to obtain the continuous phase distribution.

3. Numerical Simulation

The speckle interferograms used to evaluate the performance of the proposed phase retrieval technique were generated by computer simulation. As described before, this approach allows us to know precisely the original phase distribution and, therefore, to determine the errors introduced by the algorithm used for evaluating the phase change. For this purpose, we used a simulation method similar to the one proposed in Ref. [11], which assumes that the speckle distribution generated by the rough object is fully developed.

Considering a $4f$ optical configuration of an out-of-plane speckle interferometer, the intensity of the speckle interferogram recorded in the initial state I_a can be simulated as

$$I_a = |R\exp(j\alpha) + F^{-1}HF[\exp(j\phi_s)]|^2, \quad (13)$$

where R and α are the amplitude and phase of the reference beam, respectively, and j is the imaginary unit. ϕ_s is a random variable with uniform distribution in $(-\pi, \pi]$. F and F^{-1} denote the direct and inverse two-dimensional Fourier transform, respectively, and H is a circular low pass filter defined as

$$H(\rho) = \begin{cases} 1 & \rho \le D/2 \\ 0 & \rho > D/2 \end{cases}, \quad (14)$$

where D is the pupil diameter and ρ is the modulus of the position vector in the pupil plane.

On the other hand, the displacement produced in the deformed state can be introduced in Eq. (13) as

$$I_b = |R\exp(j\alpha) + F^{-1}HF\{\exp[j(\phi_s + \Delta\phi_o)]\}|^2, \quad (15)$$

where $\Delta\phi_o$ is the phase change generated by the deformation.

The simulated speckle distributions were generated with a resolution of 512×512 pixels and a scale of 256 gray levels. Moreover, the pupil diameter D was chosen in order to obtain an average speckle size of 1 pixel. Finally, the reference beam was added with twice ($R = 2$) the mean amplitude of the object beam and, without loss of generality, we have chosen $\alpha = 0$.

To compare the phase changes given by the proposed phase retrieval technique with the original input phase distribution, the rms phase error σ was evaluated as

$$\sigma = \left\{\frac{1}{L}\sum_{m=1}^{L}\sum_{n=1}^{L}[e(m,n) - \langle e\rangle]^2\right\}^{1/2}, \quad (16)$$

with the error matrix $e(m,n)$ defined by

$$e(m,n) = |\Delta\phi(m,n) - \Delta\phi_o(m,n)|, \quad (17)$$

where $\Delta\phi$ is the phase change between the initial and the deformed states determined with the proposed approach, $\Delta\phi_o$ is the original input phase distribution, $\langle e\rangle$ is the mean value of the matrix e, and m and n are the spatial coordinates of the pixel along the horizontal and vertical directions, respectively, with $L = 512$.

As mentioned in Section 1, the performance of the proposed phase retrieval method was also compared with the one given by the Carré phase-shifting algorithm. As it is well known, this technique involves the introduction in the object beam of the interferometer of four additional equal phase shifts γ between the successive frames [4]. Therefore, the intensity of the four speckle interferograms recorded in the initial state were simulated as

$$I_a^k = |R + F^{-1}HF\{\exp[j(\phi_s + \gamma_k)]\}|^2, \quad (18)$$

where $\gamma_k = (k-1)\gamma$ with $k = 1, \ldots, 4$.

In the deformed state, the four speckle interferograms were generated from

$$I_b^k = |R + F^{-1}HF\{\exp[j(\phi_s + \Delta\phi_o + \gamma_k)]\}|^2. \quad (19)$$

In practice, the main problem with phase-shifting algorithms is their susceptibility to errors due to miscalibrations of the phase-shifting device. A common situation is that the actual phase change γ_k differs by a small amount ε from the expected phase shift. In order to simulate more realistic experimental conditions, the phase shift values γ_k were selected as

$$\gamma_1 = 0, \qquad \gamma_2 = \gamma(1+\varepsilon),$$
$$\gamma_3 = 2\gamma(1-\varepsilon), \qquad \gamma_4 = 3\gamma(1+\varepsilon). \quad (20)$$

In the simulations, ε was chosen as 0.012 to consider a linear phase-shifter miscalibration of 1%.

4. Numerical Results

The proposed phase retrieval method was tested using three different phase distributions in which the highest phase change between the initial and deformed states was $\pi/3$. In the case of an out-of-plane tilt displacement, Fig. 1 shows the plot (bold curve) of the retrieved phase distribution obtained by the proposed approach and plotted along a direction

crossing the center of the pattern. In this case, the correlation was evaluated using a sliding window of size 65×65 pixels. For comparison, the same figure also displays the original input phase map (thin curve). In this figure, it is important to note that the proposed method does not give phase values over the first and the last $s/2$ pixels, where s is the size of the sliding window used to calculate the correlation. It must be mentioned that the selection of s depends on the shape of the phase distribution to be evaluated. A larger sliding window is usually preferred to smooth the retrieved phase map to be obtained. However, larger windows also tend to reduce small bumps that may appear in the phase map and could indicate the presence of a subsurface defect located in the object to be tested. For comparison, Fig. 1 also depicts the phase distribution (solid circles) retrieved by means of the Carré phase-shifting technique.

As mentioned in Section 3, the rms phase error σ was used to evaluate the performance of the proposed phase retrieval method. In this example, the proposed method outperforms the Carré phase-shifting technique, as it gives $\sigma = 0.0044$ rad compared to the value of 0.0092 rad that was obtained using the conventional approach.

Another typical example is shown in Fig. 2. This figure depicts the retrieved phase distribution (bold curve) of an out-of-plane parabolic displacement obtained using the proposed approach and evaluated along a line crossing the center of the pattern. In this example, the correlation was also evaluated using a sliding window of size 65×65 pixels. For comparison, the figure also shows the original input phase map (thin curve) and the phase distribution obtained using the Carré phase-shifting technique (solid circles). In Fig. 2, it is also observed that the phase distribution obtained with the proposed approach presents larger errors where the slope is smaller. In this second example, the performances of both approaches were quite similar, as the rms phase error

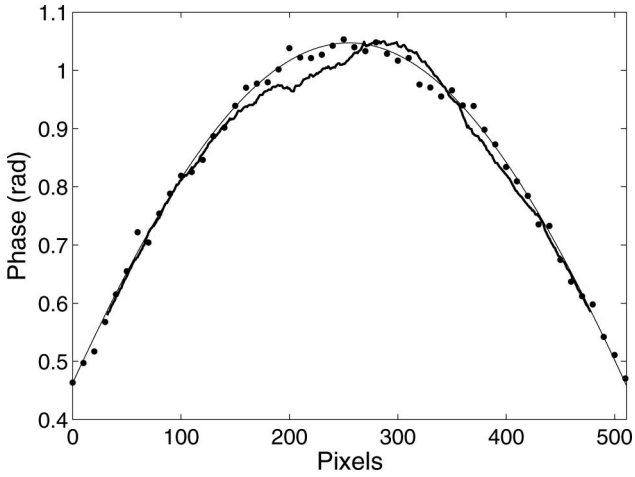

Fig. 2. Comparison between the original phase change (thin curve) with the retrieved phase maps obtained using the proposed approach (bold curve) and the Carré phase-shifting technique (solid circles) for a simulated out-of-plane parabolic displacement.

obtained with the proposed phase retrieval method was $\sigma = 0.0079$ rad and with the Carré phase-shifting technique was $\sigma = 0.0072$ rad.

The last example analyzes a more general phase distribution presenting various bumps. Figure 3 depicts the phase (bold curve) obtained by means of the proposed approach and plotted along a line crossing the center of the pattern. In this example, the correlation was evaluated using a smaller sliding window of size 21×21 pixels due to the presence of the bumps. Compared to the results obtained in previous examples, it is observed that the retrieved phase distribution generated by the proposed approach presents a lower signal-to-noise ratio due to the smaller size of the sliding window used in the computations. For comparison, this figure also displays the original input phase map (thin curve) and the phase distribution obtained using the Carré phase-shifting technique (solid circles). In this last example, the phase-shifting method shows better performance

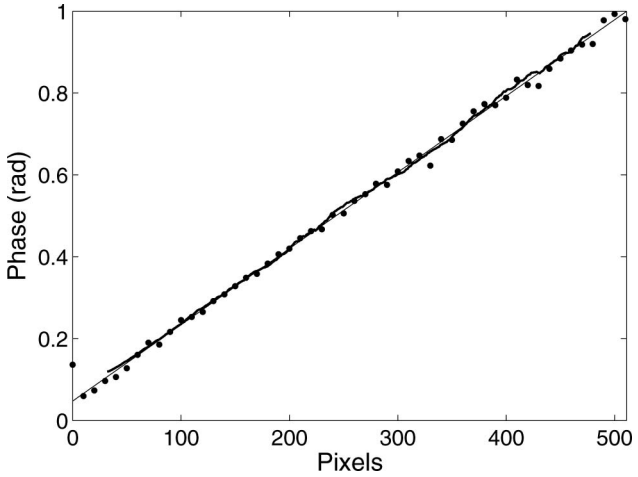

Fig. 1. Comparison between the original phase change (thin curve) with the retrieved phase maps obtained using the proposed approach (bold curve) and the Carré phase-shifting technique (solid circles) for a simulated out-of-plane tilt displacement.

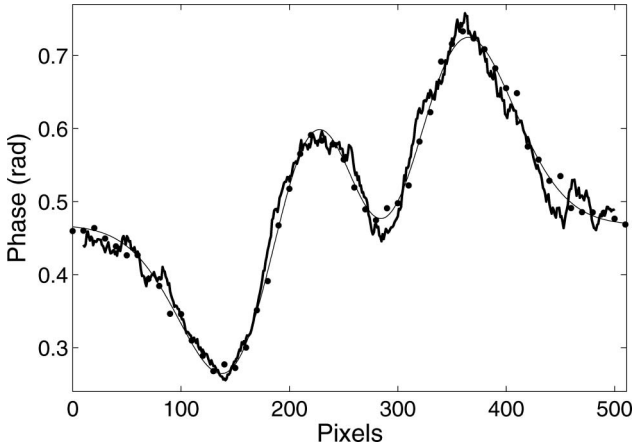

Fig. 3. Comparison between the original phase change (thin curve) with the retrieved phase maps obtained using the proposed approach (bold curve) and the Carré phase-shifting technique (solid circles) for a simulated out-of-plane generic displacement.

than the proposed approach, as this last method gave an rms phase error of $\sigma = 0.0126$ rad in comparison to $\sigma = 0.0057$ rad produced by the Carré approach.

5. Experimental Results

To illustrate the performance of the proposed phase retrieval method when experimental data are processed, a DSPI system was used to measure the out-of-plane displacement component w produced by a steel plate when it was rotated around a fixed horizontal axis using a differential micrometer. Figure 4 shows a schematic view of the out-of-plane interferometer used to record the speckle interferograms, which is similar to the one presented in Ref. [12]. This experimental setup also had a phase-shifting facility to evaluate the phase distribution using the Carré phase-shifting technique and to be compared with the phase map obtained using the proposed approach.

In order to determine the phase change $\Delta\phi$ using the proposed phase retrieval method, it was necessary to record the interferograms I_a and I_b and also the intensity of each beam that produced them. Therefore, the intensity bias and the modulation intensity for both initial and deformed states were evaluated and the correlation coefficient $C(I_a - I_{a0}, I_b - I_{b0})$ was calculated using Eq. (3). Afterward, the phase change $\Delta\phi$ was obtained by means of Eq. (12) and the out-of-plane displacement component w was finally computed as [13]

$$w = \frac{\lambda}{4\pi}\Delta\phi, \tag{21}$$

where $\lambda = 532.8$ nm is the wavelength of the Nd:YAG laser.

Figure 5 depicts the out-of-plane displacement component w measured with the proposed approach (bold curve), plotted along a line crossing the center of the steel plate. This figure shows that the maximum out-of-plane displacement generated by the plate is 30 nm. In this case, the correlation was evaluated using a sliding window of size 65×65 pixels. As mentioned in Section 4, the proposed method does not give phase values over the first and the last 32 pixels due to the size of the sliding window used to calculate the correlation. The same figure also shows the linear fit (thin curve) obtained from a least square calculation of the measured data. Despite some scatter, it is observed that this line fits quite well with the measurements. For comparison, the same figure also displays the out-of-plane displacement component obtained with the Carré phase-shifting technique (solid circles). The results shown in this last figure demonstrate that the performances given by both processing approaches are quite similar, and confirm the simplicity and accuracy of the proposed phase retrieval method to measure displacement fields in the nanometer range.

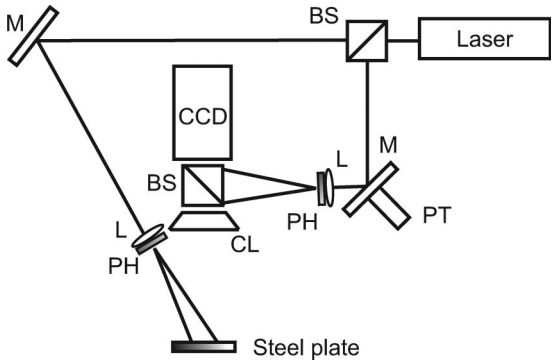

Fig. 4. Optical arrangement of the out-of-plane digital speckle pattern interferometer: Nd:Yag laser; M, mirrors; PT, piezoelectric transducer; L, microscope objectives; BS, beam splitters; PH, pin holes; CL, camera lens.

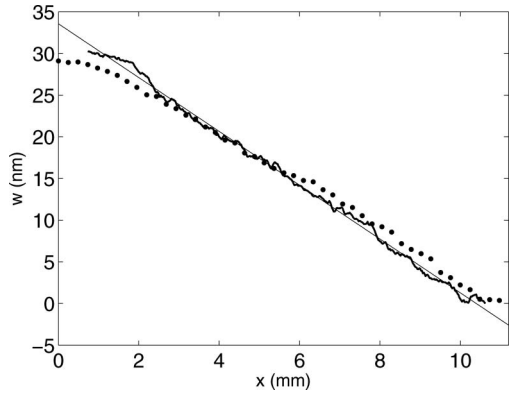

Fig. 5. Out-of-plane displacement component w along a line crossing the center of the steel plate obtained using the proposed approach (bold curve), with its linear fit (thin curve) and the Carré phase-shifting technique (solid circles).

6. Conclusions

We analyze an alternative phase retrieval method to be used in DSPI for measuring nanometric displacement fields when the correlation fringes show less than one complete fringe. The proposed phase evaluation method is based on the calculation of the correlation between the two speckle interferograms generated by both deformation states of the object. Although to determine the phase change it is necessary to record the intensity bias and the modulation intensity for both the initial and deformed states, this approach does not need the introduction of a phase-shifting facility in the optical setup. Also, the same processing approach can be used to measure phase distributions generated by in-plane and out-of-plane displacements without any sign ambiguity. The performance of the proposed method was investigated using three different computer-simulation phase distributions. As the input phase change introduced in each sequence of computer-simulated speckle interferograms is known, this approach allows us to evaluate the rms phase error introduced by the proposed method. The numerical results presented in this work show that the proposed phase retrieval method has good performance, similar to that obtained with a phase-shifting approach. The quality of the obtained results mainly depends on the size of

the sliding window used to calculate the correlation operation. In the cases where the size of the sliding window is quite large, the proposed approach outperforms the Carré phase-shifting technique. Finally, these numerical results were confirmed by processing experimental data obtained from the analysis of a steel plate when it was rotated around a fixed horizontal axis with a differential micrometer. These last results illustrate the simplicity and accuracy of the proposed phase retrieval method when the DSPI technique should be applied to test different components in the nanometer scale.

L. P. Tendela acknowledges the financial support provided by Fundación Josefina Prats of Argentina. The authors also thank the Agencia Nacional de Promoción Científica y Tecnológica of Argentina for financial support.

References

1. *Optical Inspection of Microsystems*, W. Osten, ed. (Taylor & Francis, 2007).
2. *Digital Speckle Pattern Interferometry and Related Techniques*, P. K. Rastogi, ed. (Wiley, 2001).
3. R. Höfling and P. Aswendt, "Speckle metrology for microsystem inspection," in *Optical Inspection of Microsystems*, W. Osten, ed. (Taylor & Francis, 2007), pp. 427–458.
4. J. M. Huntley, "Automated analysis of speckle interferograms," in *Digital Speckle Pattern Interferometry and Related Techniques*, P. K. Rastogi, ed. (Wiley, 2001), pp. 59–139.
5. J. M. Huntley, "Automated analysis in experimental mechanics: a review," J. Strain Anal. **33**, 105–125 (1998).
6. B. V. Dorrío and J. L. Fernández, "Phase-evaluation methods in whole-field optical measurement techniques," Meas. Sci. Technol. **10**, R33–R55 (1999).
7. *Laser Speckle and Related Phenomena*, J. C. Dainty, ed. (Springer-Verlag, 1989).
8. R. Jones and C. Wykes, *Holographic and Speckle Interferometry* (Cambridge Univ. Press, 1983).
9. D. R. Schmitt and R. W. Hunt, "Optimization of fringe pattern calculation with direct correlations in speckle interferometry," Appl. Opt. **36**, 8848–8857 (1997).
10. J. D. Dobson, *Applied Multivariate Data Analysis Volume I: Regression and Experimental Design* (Springer-Verlag, 1991).
11. G. H. Kaufmann, A. Dávila, and D. Kerr, "Digital processing of ESPI addition fringes," Appl. Opt. **33**, 5964–5969 (1994).
12. L. P. Tendela, A. Federico, and G. H. Kaufmann, "Evaluation of the piezoelectric behavior produced by a thick-film transducer using digital speckle pattern interferometry," Opt. Lasers Eng. **49**, 281–284 (2011).
13. P. K. Rastogi, "Measurement of static surface displacements, derivatives of displacements and three dimensional surface shape. Examples of applications to non-destructive testing," in *Digital Speckle Pattern Interferometry and Related Techniques*, P. K. Rastogi, ed. (Wiley, 2001), pp. 142–224.